Understanding and Forecasting Tropical Cyclone Intensity Change with the Typhoon Intensity Prediction Scheme (TIPS)

Patrick J. Fitzpatrick*

Department of Atmospheric Science, Colorado State University, Fort Collins, Colorado

ABSTRACT

A multiple regression scheme with tropical cyclone intensity change as the dependent variable has been developed. The new scheme is titled the Typhoon Intensity Prediction Scheme (TIPS) and is similar to one used operationally at the National Hurricane Center. However, TIPS contains two major differences: it is developed for the western North Pacific Ocean, and utilizes digitized satellite data; the first time such satellite information has been combined with other predictors in a tropical cyclone multiple regression scheme. It is shown that the satellite data contains vital information that distinguishes between fast and slow developing tropical cyclones. The importance of other predictors (such as wind shear, persistence, climatology, and an empirical formula dependent on sea surface temperature) to intensity change are also clarified in the statistical analysis. A normalization technique reveals threshold values useful to forecasters. It is shown that TIPS may be competitive with the Joint Typhoon Warning Center in forecasting tropical cyclone intensity change.

1. Introduction

a. Overview of intensity prediction accuracy

According to a 1987 survey of all tropical cyclone (TC) forecast centers in the world, the overriding TC research emphasis has been placed on track forecasting with little investigation on intensity change (McBride and Holland 1987). The past decade has witnessed little improvement (DeMaria and Kaplan 1994b; Elsberry et al. 1992). As a result, systematic and skillful intensity forecasting techniques have yet to be established, and much is still not understood about TC intensity change. A National Disaster Survey Report (1993) noted that hurricane intensity forecasts lack accuracy and lag far behind other forecasting applications such as track prediction. The report urges scientists to "redouble their efforts to develop models and operational techniques to forecast tropical cyclone intensity changes more effectively."

Not surprisingly, large errors occur when forecasting TC intensity. The measure of intensity forecast around the world is the maximum sustained surface wind speed (V_{max}), often tabulated in knots. The mean 24-h Joint

Typhoon Warning Center (JTWC) absolute error was 12.5 kt for intensity forecasts during 1980–85 (Mundell 1990). Furthermore, the Australian Bureau of Meteorology Research Center (BMRC) reports that their TC intensity forecasts were not even as accurate as a prediction based on persistence or climatology (Elsberry et al. 1992). DeMaria and Kaplan (1994b) noted that official National Hurricane Center (NHC) forecast skill was comparable to a regression forecast based on climatology and persistence, and only slightly better than persistence.

The largest errors in TC intensity forecasting occur with "rapidly intensifying" systems (Mundell 1990), defined as a central pressure drop of at least 42 mb day^{-1} by Holliday and Thompson (1979). (This corresponds to an approximate V_{max} increase of 45 kt day^{-1}.) Other classifications exist to delineate abrupt TC development, such as "explosive deepening" (Dunnavan 1981) defined as a 12-h central pressure drop of at least 30 mb. However, these definitions only apply to one time period (24 h) and would provide too few cases in the comparison of different intensification rates (section 4). In this paper, a broader category of "fast intensification" is used, defined as a 24-h (48-h) increase of V_{max} by 25 kt day^{-1} [45 kt (2 day)$^{-1}$] or more. As shown by Mundell (1990) and by this paper, all three classifications are associated with errors that are roughly twice the average intensity error, and result in underforecasting intensity.

b. Consequences of underforecasting TC intensity

Unanticipated fast development is currently a forecast reality. Some storms that experienced unpre-

* Current affiliation: Department of Physics, Atmospheric Sciences, and General Science, Jackson State University, Jackson, Mississippi

Corresponding author address: Dr. Patrick J. Fitzpatrick, Department of Physics, Atmos. Sciences and General Science, Jackson State University, P.O. Box 17660, Jackson, MS 39217-0460.
E-mail: patrick@stallion.jsums.edu

dicted fast intensification are Typhoon Niña (1987), which struck the Philippines, killed hundreds, and left half a million homeless (Mundell 1990); Hurricane Hugo (1989) before its South Carolina landfall; Typhoon Omar (1992) before it impacted Guam, causing $457 million in damage and grounding two navy supply ships; Hurricane Andrew (1992) before its Florida landfall, resulting in record property damage estimated at $25 billion, destroying 25 524 homes, damaging 101 241 homes, and putting eight insurance companies out of business (Mayfield et al. 1994; Sheets 1994); and Hurricane Opal (1995) the night before its Florida landfall, surprising awakening residents who congested the road systems in last-minute evacuation attempts (Fitzpatrick 1996).

It is the prospect of more such dangerous situations that motivates this paper, which describes a new multiple regression scheme for TC intensity change. Developed on western North Pacific data, this statistical analysis yields an intensity forecast scheme, which may be used as guidance in real-time operations, and also generates understanding about TC intensity change.

c. Previous TC intensification research

Theoretical intensity change work concentrates on three areas: 1) interaction with upper-tropospheric troughs and angular momentum fluxes, categorized here as "upper-level forcing"; 2) inner-core convective processes; and 3) environmental factors such as sea surface temperature (SST) and vertical wind shear. The importance of upper-level forcing has been a contentious issue in tropical meteorology (Fitzpatrick 1996). The disagreement stems from the fact that fast TC development is a relatively unusual event. One interpretation is that an "extra ingredient" must be required to enhance TC intensification, and that extra factor is upper-level forcing. The other interpretation is that the combination of warm water and low wind shear is an infrequent event and that fast TC intensification is generally more favorable in an environment free of upper-level anomalies since upper-tropospheric troughs are often associated with wind shear.

Two scenarios of trough interactions that might intensify a TC have been proposed: 1) enhancement of the storm's outflow by favorable positioning of a trough (Sadler 1978; Shi et al. 1990; Rodgers et al. 1991) and/or 2) enhancement of the storm's development through dynamical forcing, viewed in the context of differential vorticity advection and potential vorticity coupling (Montgomery and Farrell 1993). Upper-level asymmetries (eddy fluxes), which are often but not always associated with troughs, also may affect intensification. One azimuthally averaged quantity, known as the relative eddy angular momentum flux convergence (REFC), can theoretically contribute to TC development. Many researchers have attributed REFC forcing to fast TC intensification in modeling studies (Pfeffer and Challa 1980), theoretical discussions (Holland and Merrill 1984), observational studies (Molinari and Vollaro 1989; Rodgers and Pierce 1995), and statistical studies (DeMaria et al. 1993). Other eddy flux terms may also be important, such as planetary eddy angular momentum flux convergence (PEFC) (DeMaria and Kaplan 1994b; Molinari and Vollaro 1990).

In contrast with these findings, Merrill (1988) could find no relationship between REFC and intensity change. He speculated that any positive influences of upper-level forcing is usually offset by the negative influences of increased vertical wind shear associated with a trough. Merrill also stated that, in a general sense, environmental interactions must contribute negatively to intensity change since most TCs do not reach moderate to extreme intensities. Merrill noted the existence of a maximum potential intensity (MPI) as a function of SST. MPI represents an upper bound for which TCs of stronger intensity do not exist for a given SST. An example of an empirical MPI curve is shown for western Pacific TCs in Fig. 1 (Kubat 1995). Since few TCs reach their MPI (Merrill 1987; Evans 1993; DeMaria and Kaplan 1994a), Merrill argued the environment is exerting a negative influence most of the time.

The effect of SST on TC development has been known for decades (Palmén 1948). The ultimate energy source for the TC is the latent and sensible heat flux from the ocean. As air spirals into a TC, it is subjected to sea level pressure reductions that would decrease the air temperature substantially due to adiabatic expansion; however, because of ocean fluxes, an air parcel is able to (mostly) preserve its air temperature. As originally discussed by Riehl (1954), an air parcel following a mostly isothermal path toward the eyewall region and experiencing a pressure drop will obtain buoyancy as it ascends in the eyewall; this gain offsets the stabilization effect of the developing warm-core aloft. Therefore, the secondary circulation is maintained and the TC can continue to intensify through this feedback mechanism (Fitzpatrick 1996; Holland 1997). As SSTs increase, this feedback increases the MPI nonlinearly as shown in Fig. 1. As will be seen, the most important statistical TC intensity predictor is a variation of the MPI threshold.

Another important contributor to intensification may be eye formation (Fitzpatrick 1996). Typically an eye develops near hurricane strength (Dvorak 1984), and Mundell (1990) showed that most rapid intensification occurs near eye formation. Operational forecasters and researchers also have recognized that inner-core convective flare-ups indicate potentially explosive development. Indeed, several satellite forecast schemes for predicting TC intensity have been developed on the

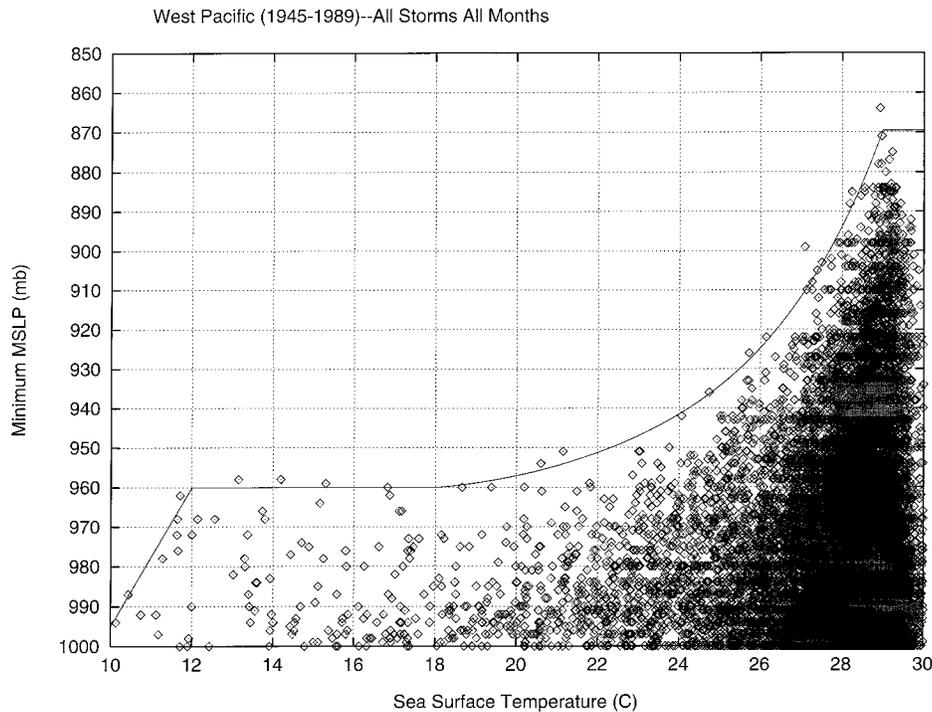West Pacific (1945-1989)--All Storms All Months

FIG. 1. The maximum potential intensity (MPI) between climatological SSTs and minimal sea level pressure for all western Pacific tropical cyclones during 1945–89. The line represents an empirical upper bound on intensity as a function of SST. A plot vs maximum sustained wind reveals a similar structure (not shown). Adapted from Kubat (1995).

premise that convective bursts precede fast intensification.[1]

d. Satellite TC intensity forecast schemes

Despite today's accessibility to satellite data, few objective TC forecasting techniques exist based on this technology. The only proven technique used operationally is a flowchart algorithm based on synoptic observations, TC structure, and TC development climatology called the "Dvorak scheme" (Dvorak 1975, 1984). The Dvorak technique contains both a current intensity analysis scheme and an intensity prediction scheme, but only the former has been consistently used operationally, and both contain some subjectivity. However, research suggests that quantitative relationships between TC intensity change and satellite convection exist which would be very useful operationally.

Gentry et al. (1980) found the cooler the mean brightness temperatures (T_b) of the cloud tops over an 8° area, the more likely V_{max} will increase in 24–36 h. From these results, regression equations were developed using T_b parameters that outperformed persistence at 24 h on independent data. Steranka et al. (1986) expanded on Gentry et al.'s research by investigating area-average T_b within 2° of the TC center. Prolonged surges of intense convection near the storm center (measured as 6-h *running means*[2]) were followed by 24-h intensification of 5 m s^{-1} or more 71% of the time. Steranka et al. also devised multiple regression equations using T_b, T_b^2, and V_{max}, which were competitive with persistence and climatology.

Mundell (1990) presented a methodology to distinguish which storms will rapidly intensify and which storms will develop at a slower rate. Mundell developed a satellite scheme which measures the degree of inner-core (within 2° of the TC center) versus outer-core (2°–6°) convection. Mundell hypothesized that high ratios of inner- versus outer-core convection indicate future rapid intensification since inner-core processes would dominate over outer-core processes. This idea was based on reconnaissance observations by Weatherford and Gray (1988) that TCs with fast outer-core winds (implying strong inertial stability) restrict inflow to the eyewall and, thereby, do not efficiently concentrate inner-core convection (Holland and Merrill 1984).

---

[1] As mentioned by one reviewer, sometimes extreme convection can indicate *arrested* development—called the "central cold cover" signal (Dvorak 1984).

[2] A running mean is an average of current and previous observations. In this paper, it refers to the average of current and previous 3-h satellite pixel counts.

Mundell smoothed the satellite data using a running mean to remove the natural oscillatory behavior of convection and to eliminate the diurnal TC convective signals (Hobgood 1986; Hallin 1991). By using climatology and defining a threshold where inner-core convection dominated outer-core convection, Mundell forecasted 7 out of 10 rapidly deepening TCs correctly in a hindcast mode. Furthermore, of the 60 nonrapid deepeners in the dataset, 59 were predicted correctly in the development set.

While Mundell's work is interesting, it possesses several problems. The threshold value seems arbitrary and lacks a physical basis, plus the development dataset is marginal in size. Furthermore, his scheme only identifies potential rapid deepeners and does not forecast intensity change. Therefore, major objectives of this study are 1) to incorporate inner-core pixel counts in an intensity forecasting scheme in a more objective manner and 2) to develop a better understanding of the role of convection in intensity change.

e. Statistical TC intensity forecast schemes

The power of multiple regression analysis is the objective selection of predictors. Only "statistically significant" predictors are chosen, the importance of each predictor may be quantitatively assessed, and the amount of explained variance R^2 may be determined. In other words, not only does multiple regression provide a forecast equation, but it generates *understanding* of intensity change processes through objective analysis.

The first intensity change regression model, developed for the Atlantic basin and based on climatology using "best-track" data,[3] was called the Statistical Hurricane Intensity Forecast, or SHIFOR (Jarvinen and Neumann 1979). The forecast equations were generated by stepwise regression using best-track TC data as input. Significant predictors include Julian day, initial storm latitude and longitude, zonal and meridional component of initial storm movement, initial intensity, and previous 24-h intensity change. SHIFOR is currently still competitive with NHC forecasts (DeMaria and Kaplan 1994b). A similar scheme for the western North Pacific was developed by Elsberry et al. (1975), and recently updated by Chu (1994), called the Statistical Typhoon Intensity Forecast model.

Since no synoptic information is included in SHIFOR, the amount of variance explained for 24-h intensity change is only about 30%. The first attempt at incorporating synoptic parameters in a multiple regression model was performed by Pike (1985). Merrill (1987) considered a much broader range of predictors (synoptic, persistence, climatology, and SST) for the Atlan-

tic. Elsberry et al. (1988) developed a regression scheme for the western North Pacific that included climatology, persistence, and synoptic predictors. Important synoptic parameters included environmental wind flows and wind shear, which were decomposed into empirical orthogonal functions. However, Elsberry did not include SST data.

DeMaria and Kaplan (1994b) expanded on Merrill's work with the Statistical Hurricane Intensity Prediction Scheme (SHIPS) for the Atlantic basin. SHIPS includes improved predictors and a larger sample. The amount of variance explained by SHIPS is about 40% at 24 h. SHIPS was tested using a jackknife procedure and showed 10%–20% improvement compared with the official forecast and SHIFOR. SHIPS is currently used as forecast guidance at NHC in the Atlantic and eastern Pacific Oceans.

Because of its promise, the SHIPS methodology will be used in this paper. A major focus of this paper is to incorporate satellite data into a multiple regression scheme, and investigate if this new information could reduce errors associated with fast intensifiers. This is the only TC multiple regression scheme that combines climatology, persistence, synoptic, satellite, and SST information with intensity change as the dependent variable. Furthermore, no scheme analogous to SHIPS currently exists in the western North Pacific.

f. Outline of this paper

From this discussion, it is clear that more research is needed on improving intensity change prediction as well as comprehending the processes involved in intensity change. This study encompasses a statistical approach to understanding and predicting TC intensity change. The dataset is presented in section 2. The statistical methodology is described in section 3. Results are presented in section 4. Case studies are shown in section 5. A summary of this paper is presented in section 6.

2. Development of TIPS

A scheme similar to SHIPS was developed for the western North Pacific basin, and is titled the Typhoon Intensity Prediction Scheme (TIPS). A unique aspect of TIPS is that digitized infrared satellite data are used as predictors. Other predictors are based on climatology, SST, persistence, and synoptic winds. Regression is performed on 12-, 24-, 36-, and 48-h forecasts.[4] It is shown that satellite data contains vital information that distinguishes between TCs that intensify fast and those that intensify at a slower rate.

TIPS is described in detail by Fitzpatrick (1996) and

---

[3] The term "best track" refers to postprocessed intensity (V_{max}) estimates and storm positions at 6-h intervals.

[4] A 60- and a 72-h scheme were not developed due to time restrictions, and because the author wanted to investigate short-term forecasting first.
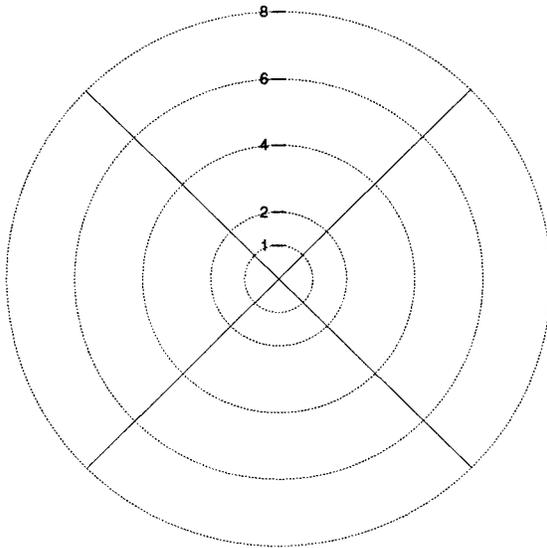
FIG. 2. Grid used for storm-centered IR data processing. Data is available between 0° and 8°. Top portion is northern quadrant, left is west, bottom is south, and right is east.

will be summarized here. Years 1983–86 were chosen for this study since the actual TC intensity was measured by reconnaissance flights. These flights were terminated in 1987, and the accuracy of TC intensity data afterward is uncertain (Martin and Gray 1993) since most TCs are primarily estimated using the satellite techniques of Dvorak (1984). The regression equations were developed for the years 1984–86, since these years contain the most data compared to other 3-yr subsets (530 cases and 66 storms for 24-h intensity change). The accuracy of the empirical scheme is tested for 1983 (139 cases and 19 storms for 24-h intensity change).

The SST data is stored by year and month on a 2° latitude and longitude grid. The data are computed as ''blended SSTs'' using the scheme of Reynolds (1988) and are interpolated to the storm center. Should a storm occur the first or last 5 days of a month, the SSTs are averaged by the current and nearest month.

The synoptic wind data is obtained from BMRC for 1984 to July 1986 (Davidson and McAvaney 1981) and from the European Centre for Medium-Range Weather Forecasts when the BMRC data is not available. Both synoptic data sources are on 2.5° grid spacing analyzed at 0000 and 1200 UTC. The synoptic parameters are interpolated to the storm center.

The satellite source is 3-h, 10-km resolution infrared ''pixels'' from three separate Geostationary Meteorological Satellites during 1983–86. Fitzpatrick (1996) explains the data processing procedure. The 512×512 pixels are centered on the best-track data and saved on a grid as shown in Fig. 2. The number of IR pixels for every brightness temperature (T_b) value was tabulated, yielding a dataset with many potential applications. In this study, a percentage of pixels colder than several T_b values for different radii are investigated for a total of

30 combinations. Thirty combinations for each set of 6-, 12-, and 24-h running means are also computed.

In summary, the 4-yr regression sample contains 0000 and 1200 UTC best-track, synoptic, SST, and satellite data with a sample size up to 600 cases. The satellite data is stored in 30 radial and T_b combinations as observed values, and as 6-, 12-, and 24-h running means. This is the first TC dataset that combines climatology, SST, synoptic, and satellite data.

Possible predictors

To assess which predictors are statistically significant, one must first define a list of ''potential predictors.'' The diagnosis of significant predictors from a pool of potential predictors is useful information by itself. For a detailed description of each potential predictor, the reader is referred to Fitzpatrick (1996). Since tropical cyclogenesis and TC intensification are separate problems (Zehr 1992), only observations in which a TC has achieved tropical storm strength ($V_{max} \geq 35$ kt) are included. This is different from SHIPS, which includes the depression stage of named TC cases.

1) CLIMATOLOGY

The climatology parameters are computed in terms of storm location, storm speed, storm direction, and time of year. Many are used in other climatology and persistence regression models for intensity change forecasts (Elsberry et al. 1975; Jarvinen and Neumann 1979; Chu 1994) and track forecasts (Neumann 1991). Although parameters related to physical processes (such as wind shear and convection) generally contain stronger forecast signals, it is found that climatology explains a proportion of the variance that these physical processes cannot. The potential climatology predictors are shown in Table 1. These include zonal (USPD) and meridional storm motion (VSPD), storm speed (SPD), storm direction (DIR), latitude (LAT), and longitude (LONG). Since some weakening storms move rapidly during recurvature, or move slowly and upwell colder water underneath (Shay et al. 1992), absolute storm speed anomaly SPDAN = |SPD − 5| is investigated with respect to the mean storm speed of 5 m s^{-1} (Weatherford 1989). Direction anomaly (DIRAN) with respect to a mean west-northwest track is also a potential predictor. Julian date anomalies with respect to the peak onset of rapid deepeners (JDAN) are included using dates cited by Mundell (1990).

Persistence with an ''eye parameterization'' (EYEPER) is also investigated as

$$\text{EYEPER} = \begin{cases} 1 & \text{if } V_{max} \geq 55 \text{ kt} \quad \text{and} \\ & \quad \Delta V_{max}(t = -12) > 0 \quad (1) \\ 0 & \text{otherwise,} \end{cases}$$

TABLE 1. Potential climatology and persistence predictors after step 1 in the screening process. Details of predictors are contained in the text. Only storms over open water with $V_{max} \geq 35$ kt are considered. Variables that were significant at the 99% level after applying steps 2 and 3 in the stepwise procedure (for at least one of the forecast intervals) are underlined.

Predictor	Description
LAT	Initial storm latitude
LONG	Initial storm longitude
SPD	Observed storm speed
SPDAN	Absolute storm speed anomaly, defined as $|SPD - 5|$ where the average storm speed is 5 m s⁻¹
DIRAN	Direction anomaly, defined as the TC direction anomaly from 310°
USPD	Zonal component of storm motion
VSPD	Meridional component of storm motion
JDAN	Anomaly from peak onset of rapid deepeners, defined as the absolute value of observed Julian day minus climatological onset of rapid intensifiers
EYEPER	Indicator variable that combines persistence with the parameterization of a well-formed, contracting eye
POT	MPI for a given SST minus initial intensity (V_{max}); MPI is averaged over the forecast track

TABLE 2. Potential synoptic regression predictors after step 1 in the screening process. Details of predictors are contained in the text. Only storms over open water with $V_{max} \geq 35$ kt are considered. Variables that were significant at the 99% level after applying steps 2 and 3 in the stepwise procedure (for at least one of the forecast intervals) are underlined. Eddy flux calculations are not in storm-relative coordinates, in contrast to Molinari and Vollaro (1990).

Predictor	Description
VWS5	Magnitude of 200–850-mb vertical wind shear averaged over a 5° circle and averaged over the forecast track; a perfect shear forecast is assumed
REFC$_{mid}$	200-mb REFC averaged between 7° and 10°
REFC$_{outer}$	200-mb REFC averaged between 11° and 15°
PEFC$_{mid}$	200-mb PEFC averaged between 7° and 10°
PEFC$_{outer}$	200-mb PEFC averaged between 11° and 15°
VORT2	200-mb vorticity in a 2.5° circle over the center of the storm
VORT5	200-mb vorticity in a 5° circle over the center of the storm
VORTADV	200-mb vorticity advection over the center of the storm

where $\Delta V_{max}(t = -12) > 0$ is the past 12-h intensity trend. Equation (1) may be interpreted as follows: when V_{max} is less than 55 kt, TCs typically do not intensify rapidly (Mundell 1990); therefore, other factors such as weak wind shear must compensate for a weak TC to intensify. Once an eye forms (typically at 55 kt), the rate of intensification increases; however, this intensification depends on the recent intensity trend. A positive trend generally indicates that the TC is early in its life cycle and that the eyewall is contracting with time. As shown by Weatherford (1989), proper consideration of the TC life cycle is important. However, a negative tendency indicates one or more of the following possibilities: 1) the TC is in the later stages of its life cycle; 2) the eye is weakening due to colder SSTs, high shear, or other adverse effects; and/or 3) the eye is experiencing a concentric eyewall cycle that is associated with temporary weakening (Willoughby 1990).[5]

Merrill (1987) found that using a modified SST variable that measures a TC's maximum "potential" future intensity change explains more variance than SST alone. This variable is based on the MPI concept shown in Fig. 1. DeMaria and Kaplan (1994a) derived the following empirical MPI relationship from a 31-yr sample of Atlantic TCs:

$$\text{MPI (kt)} = A + B \exp[-C(\text{SST}_o - \text{SST})], \quad (2)$$

where $A = 66.5$ kt, $B = 108.5$ kt, $C = 0.1813°C^{-1}$, and

SST$_o$ = 30.0°C. This research assumes Eq. (2) is valid in the western North Pacific. Like SHIPS, MPI is averaged along the future storm track during the forecast interval ($\overline{\text{MPI}}$) to account for SST variations along the track. Best-track positions are used to determine the storm positions during the forecast period. After computing $\overline{\text{MPI}}$, the modified SST variable that represents a TC's potential future intensity change (POT) is given by (DeMaria and Kaplan 1994b)

$$\text{POT} = \overline{\text{MPI}} - V_{max}(t = 0). \quad (3)$$

Should POT become negative (rare), it is set to zero, but this alteration does not change the explained variance.

2) SYNOPTIC WINDS

Several wind parameters are investigated, which some researchers consider important to intensity change. These include a variety of vorticity terms and eddy flux terms as summarized in Table 2. Another investigated parameter is vertical wind shear (VWS). The best procedure for measuring VWS has received little investigation. DeMaria and Kaplan (1994b) found that averaged shear explained slightly more variance of intensity change than traditional "single-point" shear (VWSPT) over the TC center ($r = 0$):

$$\text{VWSPT} = \{[\Delta u(r = 0)]^2 + [\Delta v(r = 0)]^2\}^{1/2}, \quad (4)$$

where $\Delta u = u_{200} - u_{850}$ and $\Delta v = v_{200} - v_{850}$ are zonal and meridional wind differences between 850 and 200 mb. To investigate whether averaged VWS is a better predictor, shear computed over a 5.0° circle (VWS5) is computed as

$$\text{VWS5} = [(\overline{\Delta u})^2 + (\overline{\Delta v})^2]^{1/2}. \quad (5)$$

Denoting the radii $r = 2.5°$ and $5.0°$ with $i = 1$ and 2,

---

[5] The previous 12-h intensity change was also investigated for persistence. The explained variance was similar to using EYEPER, but the absolute errors, particularly during the transition from intensification to weakening, were larger. This problem is associated with autocorrelation, which occurs to some extent in all regression models (Aczel 1989). The use of a "weaker" form of persistence by using the dummy variable EYEPER reduces autocorrelation.

TABLE 3. Potential pixel count regression predictors after step 1 in the screening process. Only storms over open water with $V_{max} \geq 35$ kt are considered. Variables that were significant at the 99% level after applying steps 2 and 3 in the stepwise procedure (for at least one of the forecast intervals) are underlined. One of the 30 PXRdTb combinations was chosen, as was one of the DPXRdTb combinations.

Predictor	Description
PXRdTb	Percent of infrared pixels (PX) in a radial area (Rd) colder than a specified brightness temperature (Tb) at $t = 0$; all Tb are negative; 30 combinations are investigated
PXRdTb**2	Same as PXRdTb but squared; 30 combinations are investigated
DPXRdTb	12-h trend of PXRdTb; 30 combinations are investigated
MUND	Ratio of PX0275 to PX2665
DIFFPX	PX0270 minus PX2665

and circle angle $\phi = 0°$, 90°, 180°, and 270° with $j = 1$–4, $\overline{\Delta u}$ is computed as

$$\overline{\Delta u}' = \frac{1}{9}\left[\Delta u(r = 0) + \sum_{i=1}^{2}\sum_{j=1}^{4}\Delta u_{i,j}\right] \quad (6)$$

and likewise for $\overline{\Delta v}$. Averaged wind shear over a 2.5° area (VWS2) is also investigated. Like SHIPS, VWS is averaged along the future storm track during the forecast interval to account for shear changes along the track. Best-track positions are used to determine the storm positions during the forecast period. A ''perfect-prog'' of VWS is assumed.[6]

3) SATELLITE INFRARED DATA

Thirty combinations of radial areas and brightness temperature T_b were processed. The radial areas are 0°–1°, 0°–2°, 0°–4°, 0°–6°, 1°–2°, 2°–4°, and 2°–6°. The value of T_b ranges from $-55°$ to $-80°$C in 5°C increments. This full temperature range is explored for radii within 2°, while $-55°$ to $-65°$C is studied for radial legs outside 2°. The 30 combinations represent percentage of pixels in a radial area colder than a specified T_b. As shown in Table 3, these are coded as PXRdTb, where Rd is the radial increment and Tb is the brightness temperature designation without the minus sign. For example, the percentage of pixels in a 0°–2° circular area colder than $-65°$C is coded PX0265. Other investigated parameters include squared pixel counts and 12-h pixel count trends (DPXRdTb), which signify convective change. Another potential predictor is the pixel count difference (coded as DIFFPX) between cold inner-core cloud tops (PX0270) and outer-core cloud tops (PX2665), as suggested by Handel (1990), since the gradient of T_b could be more important than just T_b.

[6] Perfect-prog refers to the use of observed future fields rather than forecast fields (which may be incorrect) in the model development phase. It will give a very optimistic assessment of model performance.

Mundell's (1990) scheme forecasts rapid intensification onset within 12 h if the inner-core convection (0°–2° with $T_b < -75°$C) increases and/or the outer-core convection (2°–6° with $T_b < -65°$C) decreases such that the ratio of inner- versus outer-core convection reaches a specified threshold. A similar version of this scheme (coded as MUND) is investigated as MUND = PX0275/PX2665. Should PX2665 be leas than 5%, it is set equal to 5% to avoid an artificially high ratio.

3. Regression methodology

For this empirical scheme, the future change of maximum wind (ΔV_{max}) is chosen as the dependent variable (consistent with SHIPS). For example, ΔV_{max} in a 24-h period would be $V_{max}(t = 24) - V_{max}(t = 0)$, and for a 48-h forecast it is $V_{max}(t = 48) - V_{max}(t = 0)$. The statistical procedure consists of several phases. First, one needs to check if the least square assumptions are met. Second, an approach in which a few ''statistically significant'' predictors are chosen from many possible predictors needs to be devised. In this approach, the detrimental effects of artificial skill and multicollinearity need to be considered. Third, the multiple regression equation should be arranged so that the predictors (which all contain different units) can be equally compared against each other, and compared at different forecast intervals.

a. Validity of linear least squares multiple regression

Certain criteria must be met before multiple regression least squares analysis can be applied (Aczel 1989). The residuals should have a normal distribution, and the variance of the residuals for each independent variable should be constant. Histogram plots of normalized residuals revealed a Gaussian distribution, and residual plots for all predictors showed relatively uniform scatter (constant variance) of the regression errors. Hence, multiple regression is a valid technique for investigating the relationship between TC intensity change and the possible predictors.

b. Screening of potential predictors

The selection of a large number of potential variables for statistical significance testing is a delicate problem. Large numbers of available predictors can result in artificial skill (Shapiro and Neumann 1984; Mielke et al. 1996). Merrill (1987) succinctly explains that for 20 potential predictors ''which were actually random variables, one (variable) would be expected to test significant at the 95% level by chance alone.'' The inclusion of many potential variables in the screening process also increases the chance that some will be correlated with each other—a problem called multicollinearity. Multicollinearity inflates the explained variance, results in counterintuitive regression coefficients, and makes as-

sessing the individual contributions of the predictors to the dependent variable difficult (Aczel 1989). The effect of multicollinearity and artificial skill is reduced by a three-step process.

The first step involved eliminating some repetitious variables, such as only including one wind shear variable (VWS5, which explains more variance than VWSPT), resulting in the following 110 potential variables: LAT, LONG, SPD, SPDAN, DIRAN, USPD, VSPD, JDAN, EYEPER, POT, VWS5, REFC$_{mid}$, REFC$_{outer}$, PEFC$_{mid}$, PEFC$_{outer}$, VORT2, VORT5, VORTADV, 30 PXRdTb's, 30 PXRdTb**2's, 30 DPXRdTb's, MUND, and DIFFPX.

Stepwise regression with a ''backward glance'' then selects the optimum number of significant predictors using a significance value of 99%. After applying stepwise regression, some of the chosen predictors contained correlations of 0.5 or higher with each other. Step 3 involves a ''filtering process'' in which multicollinearity and artificial skill is further reduced by choosing one of the correlated variables and removing the rest. Then stepwise regression is run again. The reader is referred to Fitzpatrick (1996) for more details about the three-step process.

c. Normalization of regression coefficients

It is desirable to compare the chosen predictors to ascertain their importance, yet this is difficult to accomplish when the predictors and the dependent variable contain different units. Therefore, a normalization procedure is needed for equal comparison between the variables. Denoting σ as the standard deviation of a variable, $y = \Delta V_{max}$ $\bar{x}$ as the predictor mean, and $\bar{y}$ as the mean ΔV_{max} a number k statistically significant predictors are normalized by the following regression:

$$(y - \bar{y})/\sigma_y = \sum_{i=1}^{k} c_i(x_i - \bar{x}_i)/\sigma_i. \quad (7)$$

The advantage of this approach is that the importance of a predictor may be assessed by comparing regression coefficients c_i between different variables and different forecast intervals (DeMaria and Kaplan 1994b), and that the y intercept becomes zero (Edwards 1984). As a simplistic example, if $c_i = 0.5$ for one variable and if $(x_i - \bar{x}_i)/\sigma_i = 1.0$, then that independent variable's contribution to intensity change will be one-half of ΔV_{max}'s standard deviation plus $\bar{y}$. Should that same variable's c_i be larger for 48-h regression, then that variable is more important for 48-h forecasts than 24-h forecasts (relative to other chosen predictors).

In addition, $\bar{x}_i$ may be interpreted (to a first approximation) as a ''threshold'' value that distinguishes between intensification and weakening. Since $\bar{y}$ is small in this dataset (it ranges from 1 to 3 m s^{-1}), for a positively correlated predictor ($c_i > 0$), $x_i > \bar{x}_i$ is associated with intensification, and vice versa for $x_i < \bar{x}_i$. Similarly, if a predictor is negatively correlated ($c_i < 0$), above-

TABLE 4. Normalized regression coefficients for the combined climatological, persistence, satellite, and synoptic data for the TIPS forecast periods of 12, 24, 36, and 48 h. Variables not important at the 99% level are labeled NA (not applicable). Also shown is each predictor's mean value for the forecast periods. The units are m s^{-1} for POT, VWS5, and VSPD; percent for PX0455 and DPX0165; and °E for LONG. Here, R^2 (the coefficient of determination) is the percent of the total variance explained by the regression and n is the sample size for 1984–86.

Variable coefficients (c_i)	12 h	24 h	36 h	48 h
POT	+0.46	+0.60	+0.67	+0.68
PX0455	+0.27	+0.30	+0.30	+0.26
EYEPER	+0.31	+0.28	+0.25	+0.21
VWS5	−0.18	−0.26	−0.29	−0.27
DPX0165	+0.16	NA	NA	NA
VSPD	+0.09	+0.14	+0.13	NA
LONG	NA	NA	NA	+0.10
Variable mean ($\bar{x}_i$)	12 h	24 h	36 h	48 h
POT	38.9	38.8	38.9	39.0
PX0455	24.6	25.5	26.2	26.8
EYEPER	0.37	0.38	0.39	0.40
VWS5	8.5	8.4	8.4	8.5
DPX0165	−0.9	NA	NA	NA
VSPD	2.2	2.0	1.8	NA
LONG	NA	NA	NA	137.3
R^2 (%)	46.5	52.2	59.0	60.0
n	611	530	459	397

(below-) average values of x_i correspond to weakening (intensification).

4. Regression results

a. The significant predictors

After the filtering and stepwise procedures are completed, five to six significant predictors are chosen. Table 4 shows the normalized regression coefficients c_i from Eq. (7) for the selected predictors during the 12-, 24-, 36-, and 48-h forecast intervals. Correlation matrix calculations, and a quantity called the ''variance inflation factor'' (which measures the inflation of R^2 due to multicollinearity), both indicated that multicollinearity was small. Therefore, each predictor contains a unique relationship to ΔV_{max}.

The predictors in Table 4 are ordered by the magnitude of the regression coefficient. The four most critical predictors are (listed in importance): POT, PX0455, EYEPER, and VWS5. This shows that including satellite information is a crucial component in forecasting intensity change. The fact that the SST term POT term is most important is not surprising, but now its significance has been quantitatively measured. To graphically demonstrate these magnitude differences, bar plots of c_i are shown for the 24-h predictors (Fig. 3) and the 48-h predictors (Fig. 4).

POT is 1.5 times more important than EYEPER and PX0455 at 12 h, and 2 to 3 times more important than

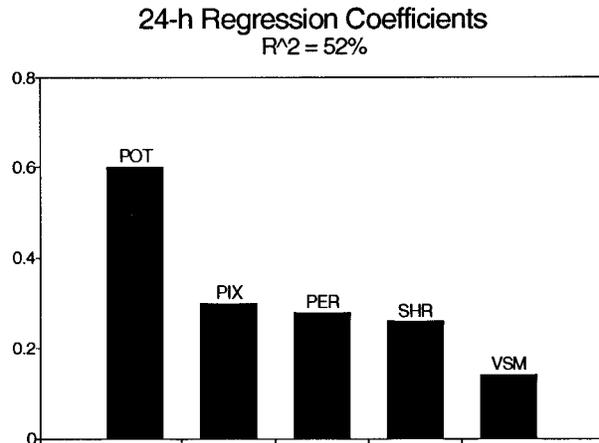## 24-h Regression Coefficients
R^2 = 52%

FIG. 3. Normalized regression coefficients for 24-h TC intensity change for the statistically significant variables. The important variables are potential intensification as a function of SST and current intensity (POT), percentage pixel counts within 4° in which $T_b <$ −55°C (PIX), persistence with an eye parameterization (PER), 5° averaged vertical wind shear (SHR), and meridional storm motion (VSM). The variance explained is 52%.

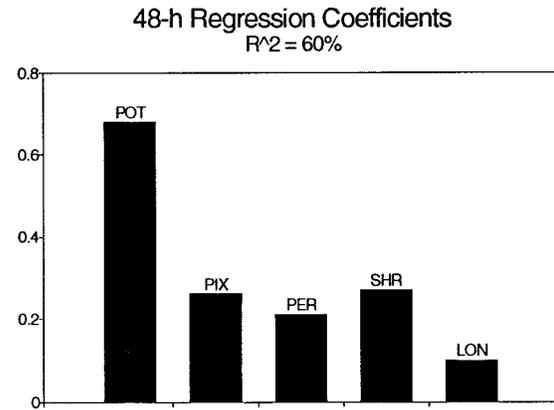## 48-h Regression Coefficients
R^2 = 60%

FIG. 4. Normalized regression coefficients for 48-h TC intensity change for the statistically significant variables. The important variables are POT, PIX, PER, SHR, and longitude (LON). The variance explained is 60%.

the other parameters. POT becomes more important for the longer forecast times (from +0.46 at 12 h to +0.68 at 48 h), and the coefficient is 2 to 5 times larger than other predictors. In general, it can be stated that *TC intensification based on potential intensity* [$\overline{MPI(SST)}$ − V_{max}] *is 2 to 3 times more important than any other predictor*. DeMaria and Kaplan (1994b) reached similar conclusions with SHIPS, although TIPS's coefficients tend to be larger. This suggests that POT might be more important in the western North Pacific than the Atlantic. However, DeMaria and Kaplan used climatological SSTs rather than observed SSTs, which could also reduce c_i.[7]

However, in general SSTs should be not interpreted as the most important predictor for intensifying TCs because the western North Pacific Ocean is uniformly 28°–29°C south of 25°N. The skill of POT may be based upon the climatology of TC intensification in that region instead, in which TCs generally develop along their track and are less likely to intensify as the MPI is approached. Then, as a TC moves toward colder water, they tend to parallel the MPI threshold (M. Landers 1997, personal communication).

The importance of PX0455 does not change much with the forecast interval, and it is the second most important predictor except for the 12-h eye/persistence term (which becomes less consequential with time). It is hypothesized that convection out to 4° embodies several influential processes, which relate to intensity change. First, it is a measure of deep inner-core con-

vection (within 0°–2°), which concentrates cyclonic vorticity through conservation of absolute angular momentum processes. Second, it is a measure of cloud symmetry; asymmetric clouds or lack of large-scale cloudiness are signs of an unhealthy storm, usually due to an unfavorable environment (shear or dry air intrusion) or due to movement over colder water. Third, the "spreading out" of cloudiness is a sign of a vigorous secondary circulation. Dvorak (1984) shows that a central dense overcast tends to form right before hurricane intensity is reached and persists during the storm's evolution as long as other conditions are favorable. In addition to these physical processes, the highest correlation to 4° may also be due to errors in the location of the TC center.[8]

It should be noted that mature, steady-state TCs may also contain deep symmetric convection and a vigorous transverse circulation. Such storms are approaching their MPI or are experiencing another influence that is restricting their development but not damaging it (such as moderate wind shear). *The intensity change predictors must be considered collectively, not by themselves.*

Wind shear averaged over a 5° area is equally as important as convection from 24 to 48 h. This suggests that shear on the edge of a TC apparently affects intensity change. It may also signify that a TC is about to enter a 200-mb westerly (or strong easterly) wind regime, or that westerly (or strong easterly) winds are about to traverse over a TC. Averaging also reduces any erroneous wind observations, bogused vortexes associated with some models, and other large-scale TC circulations from contaminating the shear calculations. It

---

[7] SHIPS began using weekly SST analyses in 1996 (M. DeMaria 1997, personal communication).

[8] Sensitivity tests were performed with other pixel count variables with different T_b radii to confirm that PX0455 was the best choice. These experiments also showed running means explained less variance than observed pixel counts. These results, as well as sensitivity tests with wind shear variables, are discussed in the appendix.

is unknown, however, if 5° averaged shear is the best shear variable for current models that have better resolution than the mid-1980s models. Elsberry and Jeffries (1996) have also shown that distinguishing between ''deep'' and ''shallow'' upper-tropospheric westerlies gives a better shear assessment, which Eq. (5) cannot compute.

Other predictors are only significant at certain forecast times. At 12 h, the DPX0165 term is the fifth most important term. Since DPX0165's components are the 12-h tendency of $T_b < -65°C$ in a 0°–1° area, it is a measure of deep inner-core convective change. The other two predictors are climatology terms. At 48 h, the storm longitude is a useful intensity change indicator. This is opposite of SHIPS, which finds LONG only to be important at 12 and 24 h, and an indication that the Pacific and Atlantic basins contain different climatologies.

A surprising finding is that the other climatology variable, meridional storm speed (VSPD), is a significant and *positive* contributor to intensity change. This somewhat bewildering discovery is contrary to SHIPS, which finds VSPD to be insignificant in the Atlantic. Once again, the basins exhibit different climatology. The reason for this result is unclear, but some tentative explanations are offered below.

According to M. Landers (1997, personal communication), in the western North Pacific during the summer, northward motion does not bring TCs over significantly colder water until 25°N, and they often do not encounter shear until about 30°N. TCs may also form fairly close to the equator, occasionally even near 5°N, and thus low-latitude TCs can contain a poleward translation component for a large distance. It is also possible the reported V_{max} contains the storm motion component, and in some accelerated recurving situations may strongly counteract the weakening influence of colder SSTs and wind shear.

To complement these findings, partial correlations for each significant variable are shown in Table 5. The partial correlation (r_p) measures how much variance is explained by one predictor when the other predictors are ''held constant'' (Edwards 1984). The same patterns in Table 4 persist in Table 5. This alternate perspective shows that, for the same persistence, convection, wind shear, and climatology values, a change in POT along the tracks will have the most profound effects, with r_p ranging from 0.5 to 0.71 (25%–49% variance). Similarly, for other predictors held fixed, the variance explained by EYEPER is about 9%–13%, for PX0455 11%–18%, and for VWS5 5%–15% while other variables affect the partial variance less.

The total variance (R^2) of intensity change explained by TIPS is 46% at 12 h and increases with each forecast interval to 60% (Table 4). Computations based on the research of Mielke et al. (1996) show that R^2 is close to the population variance (not shown) and is representative of the true explained variance. The variance in-

TABLE 5. Partial correlations for the TIPS forecast periods of 12, 24, 36, and 48 h. Partial correlations measure how much variance is explained by one predictor when the other predictors are ''held constant.'' Variables not important at the 99% level are labeled NA (not applicable).

Partial correlations	12 h	24 h	36 h	48 h
POT	+0.50	+0.63	+0.69	+0.71
PX0455	+0.33	+0.39	+0.42	+0.37
EYEPER	+0.37	+0.36	+0.34	+0.31
VWS5	−0.22	−0.33	−0.39	−0.38
DPX0165	+0.20	NA	NA	NA
VSPD	+0.11	+0.18	+0.19	NA
LONG	NA	NA	NA	+0.16

crease is due to several reasons. First, this variance increase with forecast time represents the growing importance of POT along the storm track in explaining ΔV_{max}. Second, this increase might result from the 5-kt discretization of V_{max} the best-track dataset (DeMaria and Kaplan 1994b). For intensity change in 12 h σ_y is 10 kt and increases to 28 kt at 48 h. However, the mean ΔV_{max} only slightly increases from 1.5 kt to 5 kt, respectively. This 5-kt truncation makes explaining R^2 more difficult at shorter forecast intervals since σ_y is within the noise level.[9] Finally, the lower R^2 may indicate that that inner-core processes that cannot be resolved on the synoptic scale complicate short-term intensity changes.

A discouraging finding is that 55% to 40% of the variance is still unexplained by TIPS. This accentuates the difficulty of forecasting intensity change. There is still much room for improvement in TC intensity forecasting. However, the utilization of quantitative satellite data seems promising, and its potential will become more evident as this paper continues.

Furthermore, multiple regression is a better approach than single variable linear regression. Several components must be considered when making a TC intensity forecast. To highlight these differences, Table 6 shows the variance explained in a linear, one-variable regression model (r^2). The variance explained by a single variable is astonishingly low. Even POT only explains 15%–38% by itself. The other variables explain even less variance. In fact, some values of r^2 are so small (such as for LONG, VSPD, EYEPER, and PX0455) they would typically be dismissed as unimportant if considered by themselves.

b. Threshold values

Table 4 shows the mean predictor value $\bar{x}_i$ from Eq. (7), which can be interpreted (to a first approximation)

---

[9] The value of σ_y is slightly smaller in the Atlantic than the western North Pacific. This implies that R^2 could be a little higher in TIPS than SHIPS since there is more ΔV_{max} variance to explain in the western North Pacific (M. DeMaria 1994, personal communication).

TABLE 6. Variance explained in a linear, one-variable regression model for the forecast periods of 12, 24, 36, and 48 h. Whether a variable is a positive or negative correlation is indicated. Variables not important at the 99% level in the multiple regression analysis are labeled NA (not applicable).

Single predictor variance	12 h	24 h	36 h	48 h
POT	+15.4	+23.7	+32.1	+38.1
PX0455	+10.8	+7.9	+5.6	+3.0
EYEPER	+11.2	+7.2	+4.1	+1.6
VWS5	−9.9	−11.1	−12.9	−13.0
DPX0165	+9.2	NA	NA	NA
VSPD	+2.8	+1.3	+0.9	NA
LONG	NA	NA	NA	+1.4

1) average predictor value for a class (designated as $\overline{xc}$);
2) average normalized standardized deviation ($[\overline{xc} - \overline{x}]/\sigma$) for a class, designated as NSD; and
3) whether $\overline{xc}$ is a positive influence [P; (sign of regression coefficient) $\times$ NSD ≥ 0.2], negative influence [N; (sign of regression coefficient) $\times$ NSD ≤ -0.2], or "zero" influence (Z; NSD $< |0.2|$).

This methodology is shown in Tables 7 and 8 for 24 and 48 h, respectively.

One would expect that, on average, there would be positive contributions to the intensification classes, and negative influences on the weakening classes, with zero inducements for the quasi-steady-state classes. Furthermore, one would expect large NSD differences between rapidly and slowly developing classes. Indeed, these are the general patterns, but there are some notable exceptions that reveal much about TC intensity change.

Note that the POT NSD and $\overline{xc}$ values are not very different between the fast and slow intensification classes. For example, at 24 h (Table 7) the fast and slow POT $\overline{xc}$ values are 44.2 and 46.6 m s^{-1}, respectively. Since average POT is not very different between the fast and slow developing cases, POT cannot distinguish whether a TC will develop rapidly or slowly, even though it is a positive contributor to both classes. Bar graphs are plotted in Fig. 5 for the 24-h classes to highlight this point, with the 24-h POT sample mean shown as reference.

In stark contrast, the average pixel count values are very different between fast and slow intensification cases. At 24 h, the NSD for PX0455 is 0.75 greater ($xc = 37.9\%$ compared to 26%), and in fact, on average PX0455 makes zero contribution to intensity change for the slow class. This trend is evident for the other forecast periods as well. Therefore, including pixel count information can distinguish whether a TC will develop at a fast or slow rate, and is a valuable component of TIPS. Figure 6 shows bar plots for the 24-h PX0455 classes, with the sample mean shown as reference. It is clear that abundant buoyancy is an integral part in fast developing TCs, while slower developing storms contain less buoyancy on average.

Opposite conclusions are reached for the slow and fast weakening cases. While both predictors contribute

as the threshold value for intensification and for weakening. Unlike c_i, these do not vary much for different forecast intervals. Some interesting issues emerge. First, the 5° averaged wind shear threshold of 8.5 m s^{-1} is less than the 12.5 m s^{-1} threshold for "point shear" used by Zehr (1992) in his tropical cyclogenesis study. Zehr's threshold was determined observationally and was applied to genesis. The SHIPS's threshold shear value is virtually the same 8.5 m s^{-1} as TIPS's (M. DeMaria 1995, personal communication). This suggests that the 8.5 m s^{-1} criteria for TC intensity change is probably representative of all tropical basins.

Second, the POT threshold of 39 m s^{-1} is a statement that most storms do not reach their MPI. However, this also presents forecast problems. Since TCs rarely reach their MPI, TIPS underforecasts TCs approaching the MPI limit because POT skews ΔV_{max} toward lesser values unless the other terms strongly contribute.

c. Predictor contributions to intensity change stratifications

Another feature that can be studied is how a predictor contributes to different magnitudes of ΔV_{max}. To study these stratifications, ΔV_{max} are divided into five categories: 1) fast intensifying, 2) slowly intensifying, 3) quasi-steady state, 4) slowly weakening, and 5) fast weakening. The magnitudes of ΔV_{max} that qualify for these categories have been intuitively chosen and are dependent on the forecast interval of interest. The contributions of the predictors are measured in three ways:

TABLE 7. Normalized predictors (and their true numerical values in parentheses) for different intensity regimes (kt) during the 24-h periods for 1984–86. Here, "P" denotes a positive contribution to intensification for that stratification, while "N" denotes a negative contribution; "Z" denotes zero contribution, defined as when the normalized standard deviation is less than the absolute value of 0.2. Details are contained in the text. The units are m s^{-1} for POT, VWS5, and VSPD, while PX0455 is in percent.

Variables	$\Delta V \geq 25$	$20 \geq \Delta V \geq 10$	$5 \geq \Delta V \geq -5$	$-10 \geq \Delta V \geq -20$	$\Delta V \leq -25$
POT	+0.38 (44.2) P	+0.54 (46.6) P	+0.04 (39.3) Z	−0.54 (31.0) N	−1.33 (19.6) N
PX0455	+0.78 (37.9) P	+0.03 (26.0) Z	−0.12 (23.7) Z	−0.27 (21.3) N	−0.19 (22.6) N
EYEPER	+0.51 (0.63) P	+0.07 (0.41) Z	+0.02 (0.39) Z	−0.32 (0.23) N	−0.26 (0.26) N
VWS5	−0.33 (7.0) P	−0.28 (7.2) P	+0.01 (8.5) Z	+0.25 (9.6) N	+0.90 (12.5) N
VSPD	−0.04 (1.8) Z	−0.04 (1.9) Z	−0.07 (1.8) Z	+0.00 (2.0) Z	+0.53 (3.2) P

TABLE 8. As in Table 7 but during the 48-h periods for 1984–86. The units are m s^{-1} for POT and VWS5, percent for PX0455, and °E for LONG.

Variables	$\Delta V \geq 45$	$40 \geq \Delta V \geq 20$	$15 \geq \Delta V \geq -15$	$-20 \geq \Delta V \geq -40$	$\Delta V \leq -45$
POT	+0.69 (49.2) P	+0.56 (47.2) P	+0.05 (39.8) Z	−0.84 (26.7) N	−2.1 (7.8) N
PX0455	+0.69 (37.6) P	+0.04 (27.5) Z	−0.15 (24.4) Z	−0.04 (26.2) Z	−0.18 (24.0) Z
EYEPER	+0.23 (0.51) P	+0.05 (0.42) Z	+0.02 (0.41) Z	−0.14 (0.33) Z	−0.48 (0.17) N
VWS5	−0.53 (6.4) P	−0.35 (7.1) P	+0.06 (8.7) Z	+0.47 (10.3) N	+0.66 (11.1) N
LONG	+0.41 (143.2) P	+0.04 (137.9) Z	−0.09 (136.1) Z	−0.12 (135.6) Z	+0.27 (141.3) N

negatively to the weakening classes, POT is the key predictor for differentiating between a fast and a slow disintegrating TC; PX0455 does not make this distinction. The average NSD POT difference between fast and slow weakening regimes is dramatically different, with differences of 0.57 for 12 h (−0.47 in slow weakening class compared to −1.04 in fast weakening class; not shown) and steadily increasing with the forecast interval to a NSD difference of 1.26 at 48 h in Table 8 (−0.84 in slow weakening class compared to −2.1 in fast weakening class).

The binary eye/persistence term makes a valuable distinction to all the fast and slow classes at 12 h (not shown) and the weakening classes at 48 h. However, EYEPER suffers oscillatory problems at other periods, as is evident from the fact that the class mean hovers between 0.4 and 0.5. It is because of this oscillatory fashion that EYEPER drops in importance from second to fourth place after 24 h and only makes slight contributions in the extreme ΔV_{max} classes afterward.

Wind shear adheres to the same trend as POT, in that the mean values for the fast and slow intensification classes are not acutely different, yet the NSD is markedly different between the fast and slow weakening classes. The following NSD values are observed for slow and fast weakening, respectively: 0.21 compared to 0.95 at 12 h (not shown), 0.25 compared to 0.90 at 24 h, 0.38 compared to 0.93 at 36 h (not shown), and 0.47 compared to 0.66 at 48 h. Therefore, while low shear is a vital component for intensification, on average it does not distinguish between fast and slow developing TCs. On the other hand, shear is a crucial parameter for differentiating between fast and slow weakeners on average.

The pixel count trend information (DPX0165) for 12-h forecasts contain the same NSD values for fast and slow developing classes (not shown). But, the slow and fast weakening classes exhibit markedly different NSD values, which corresponds to an average 12-h decrease of 7% and 21%, respectively. On average, the pixel count trend of deep inner-core convection does not differentiate between fast and slow 12-h developers, but does convey knowledge about when fast V_{max} decrease might occur. If PX0165 has decreased by at least 20% in the past 12 h, then V_{max} might decrease by 15 kt or more in the next 12 h.

The two climatology predictors also exhibit informative trends once stratified. The meridional storm motion only contributes significantly in the fast weakening class. For 48-h forecasts the initial storm longitude only
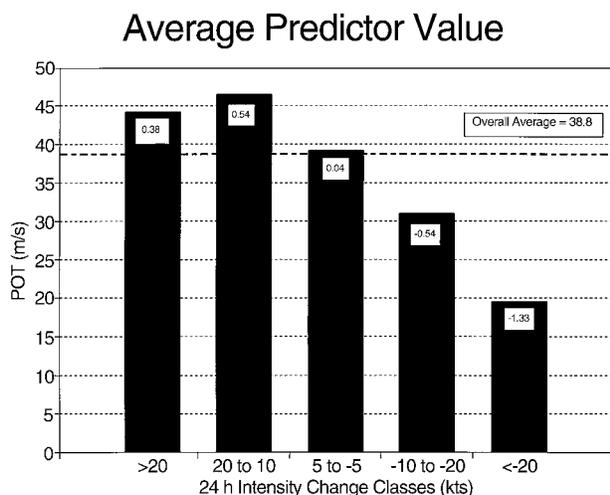

FIG. 5. Average POT values for different 24-h ΔV_{max} classes. Numbers on the bars are normalized standard deviations (NSD) defined by $(\overline{xc} - \overline{x})/\sigma$, where $\overline{xc}$ is the average POT value for each class. The overall average ($\overline{x}$, denoted by the dashed line) is shown for comparison.

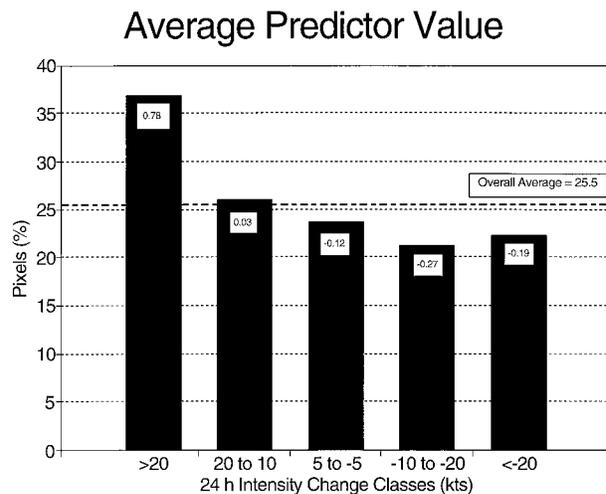FIG. 6. Average PX0455 values for different 24-h ΔV_{max} classes. Numbers on the bars are NSDs defined by $(\overline{xc} - \overline{x})/\sigma$, where $\overline{xc}$ is the average PX0455 value for each class. The overall average ($\overline{x}$, denoted by the dashed line) is shown for comparison.

contributes significantly to fast developers, with a mean location of 143.2°E.

In summary, except for EYEPER at 12 and 24 h, the observed pixel count information is the critical element in differentiating fast and slow developing TCs. Certainly warm SSTs and weak shear provide the necessary environment for fast development, but only after intense convection over a large circular area has been generated will accelerated development occur. Abundant buoyancy (convective bursts) indeed appears to be the required agent for fast development. On the other hand, cold SSTs and strong shear appear to be the main processes by which fast TC dissipation occurs; a finding that comes as no surprise.

d. Evaluation of TIPS intensity forecasts

The relative errors (biases) and absolute errors are analyzed on the dependent (1984–86) and independent (1983) dataset for TIPS and compared against JTWC's 24-h and 48-h official forecasts. (JTWC does not perform 12- or 36-h forecasts). These errors are tabulated for different ΔV_{max} classes and as an overall average. Relative error is computed as ΔV_{max} (observed) minus ΔV_{max} (forecast).

Table 9 shows the 24-h relative and absolute errors for 1984–86 and 1983. Both JTWC and TIPS suffer the same forecast biases in 1984–86. Fast intensification is underforecast, slow intensification and quasi-steady state is generally well anticipated (residuals 3 kt or less), ΔV_{max} (forecast) is less in magnitude than ΔV_{max} (observed) for slow weakening, and much less in magnitude for fast weakening. On the independent dataset, this general trend in the biases continues, although TIPS fairs better in the fast intensification, slow intensification, and fast weakening classes,—and worse in the other classes—than JTWC. In terms of absolute error, JTWC and TIPS are equal for fast intensification in 1984–86, and JTWC is slightly better in 1983 for the slow weakeners. Otherwise, all other parameters in 1984–86 and 1983 show less absolute error for TIPS despite its biases.

In general, the regression errors are fairly high but are 19% less on average compared to JTWC, 35% less for the slower intensifiers, and 20%–23% less for fast categories of ΔV_{max}. On the other hand, TIPS faired worse than JTWC for the slow weakeners in 1983, indicating that TIPS often misses the transition from an intensifying to a weakening storm. The persistence term is partially responsible for this error.

The same error patterns persist at 48 h, but the error differences are larger at 48 h, as indicated in Table 10. This does not suggest that TIPS' perfect-prog 48-h forecasts have more skill than the 24-h version, but reflects that JTWC's 48-h forecasts contains more errors due to uncertainty in track and shear predictions than their 24-h forecasts. However, the fact that the bias is 17 kt less for both 1983 fast and slow intensifying cases, with a

4.3-kt bias for the slow intensifier, is very encouraging. The errors are still unsatisfactory, but since it has been demonstrated that the satellite information is a key factor in discriminating between fast and slow intensifiers, future error reductions may be possible using satellite information in similar schemes.

e. Overall assessment of TIPS compared to JTWC

It cannot be claimed that TIPS outperformed JTWC. TIPS is developed assuming a perfect-prog of storm motion and shear. Certainly some of the JTWC errors resulted from bad track forecasts and to uncertainty in the wind shear evolution. TIPS is also developed on postprocessed (best-track) data. Sometimes the position and motion of a TC is uncertain, and operational data may contain errors that affect the forecaster's judgment. However, DeMaria and Kaplan (1994b) compared SHIPS's results developed on track forecasts based on Vic Ooyama's nested barotropic hurricane track forecasting model (VICBAR) to those developed on best-track data and found little difference in the forecast errors. They reasoned that since MPI and shear are averaged along the track, the impact of track errors is reduced. Shear and MPI are also computed this way in TIPS.

Forecasting wind shear is a daunting problem, though. The tropical upper-troposphere is subject to a variety of westerly wind intrusions from the midlatitudes and trough interactions, which are difficult to predict. Unfortunately, models offer little wind shear guidance. Numerical model forecasts of 200-mb tropical winds can be erroneous, especially in the vicinity of the Tropical Upper-Tropospheric Trough (TUTT), which tends to be artificially weakened in some models (Fitzpatrick et al. 1995).[10] Another complicating factor is that TCs can create a region of low shear with a well-developed upper-level anticyclone that can drive away a high shear environment, and this situation cannot be easily anticipated (Elsberry and Jeffries 1996). Because of these reasons, shear is often inaccurately predicted. Using perfect-prog shear will give an overestimate of TIPS's true forecast skill.

Nonetheless, TIPS may be competitive with JTWC since all the errors were similar or less in magnitude. The intensification classes where the error differences are statistically significant are shown in Tables 9 and 10, indicating where *potentially* the biggest gains could be attained.[11] TIPS can possibly provide forecast guid-

---

[10] Fitzpatrick et al. (1995) offer tips on predicting wind shear near a TUTT.

[11] This is misleading, though, because in addition to the other problems mentioned in this section, *t* numbers are inflated by autocorrelation as well.

TABLE 9. Average 24-h errors (in kt) for the regression model and JTWC forecast for the dependent dataset (1984–86) and independent dataset (1983). The errors are stratified by intensity change regimes. Number of cases for all stratification is also shown. Since JTWC released fewer forecasts than was empirically analyzed, there are fewer cases in the error analysis (514) than in Table 4 (530). Error differences significant at the 90%, 95%, and 99% levels are indicated as *, **, and ***, respectively. Errors are computed as ΔV_{max} (observed) minus ΔV_{max} (forecast). TIPS is developed on perfect-prog forecasts of shear and track, and on postprocessed data that contain some autocorrelation, so this table does not imply that TIPS can outperform JTWC.

Years	$\Delta V \geq 25$	$20 \geq \Delta V \geq 10$	$5 \geq \Delta V \geq -5$	$-10 \geq \Delta V \geq -20$	$\Delta V \leq -25$	Overall
		Mean 24-h relative errors				
1984–86 TIPS	+16.1	+3.8*	−2.1	−7.2	−13.4	0.0
1984–86 JTWC	+16.3	+2.1	−2.9	−6.7	−13.0	−0.6
1983 TIPS	+21.1	+2.0***	−6.2**	−8.8**	−14.2	−1.6***
1983 JTWC	+25.5	+8.7	0.7	−4.6	−17.7	+3.2
		Mean 24-h absolute errors				
1984–86 TIPS	16.7	7.2**	6.6***	9.3*	13.4	9.2***
1984–86 JTWC	16.7	8.8	10.5	11.0	15.3	11.3
1983 TIPS	21.1**	8.4***	9.0	11.3	14.2	11.8***
1983 JTWC	27.5	13.0	11.8	10.5	17.7	14.6
		No. of cases				
1984–86 cases	66	146	148	119	35	514
1983 cases	20	35	28	39	13	135

ance, especially when its biases are understood by the forecaster. Furthermore, besides developing a forecast scheme, an equally important scope of this research is to better understand TC intensity change, which is best analyzed using perfect-prog.

f. Comments on insignificant predictors

While the significant predictors are of most concern in this paper, it is equally illuminating to note which predictors were not significant, especially since many of the unchosen potential predictors are considered to be very important to TC intensity change by some researchers. For example, the upper-level forcing terms REFC and 200-mb vorticity advection (VORTADV) were considered statistically insignificant in the regression analysis. This concurs with the discussion of Merrill (1988) and many operational forecasters who state that any positive benefits associated with these terms

usually are overwhelmed by the corresponding negative effects of vertical wind shear that often accompanies a trough. Statistically insignificant variables are shown in Tables 1–3 *without* underlines.

5. Case studies

To complement these findings, case studies of typhoons will be shown with the emphasis on 24-h intensity change. As stimulation for discerning why some TCs intensify at a fast rate, why some intensify at a slower rate, and why some do not develop much at all, a fast developer (Lola 1986) will be investigated first (Fig. 7). As a reference frame for this and other discussions in this section, the time series are plotted from day 0 of the TC (usually its depression phase) with the date shown in the figure. MPI and V_{max} are plotted in 0.25-day (6-h) increments. VWS5 and PX0455 are plotted in 0.5-day (12-h) increments. Threshold values for

TABLE 10. As in Table 9 but for 48-h errors. TIPS is developed on perfect-prog forecasts of shear and track, and on postprocessed data that contain some autocorrelation, so this table does not imply that TIPS can outperform JTWC.

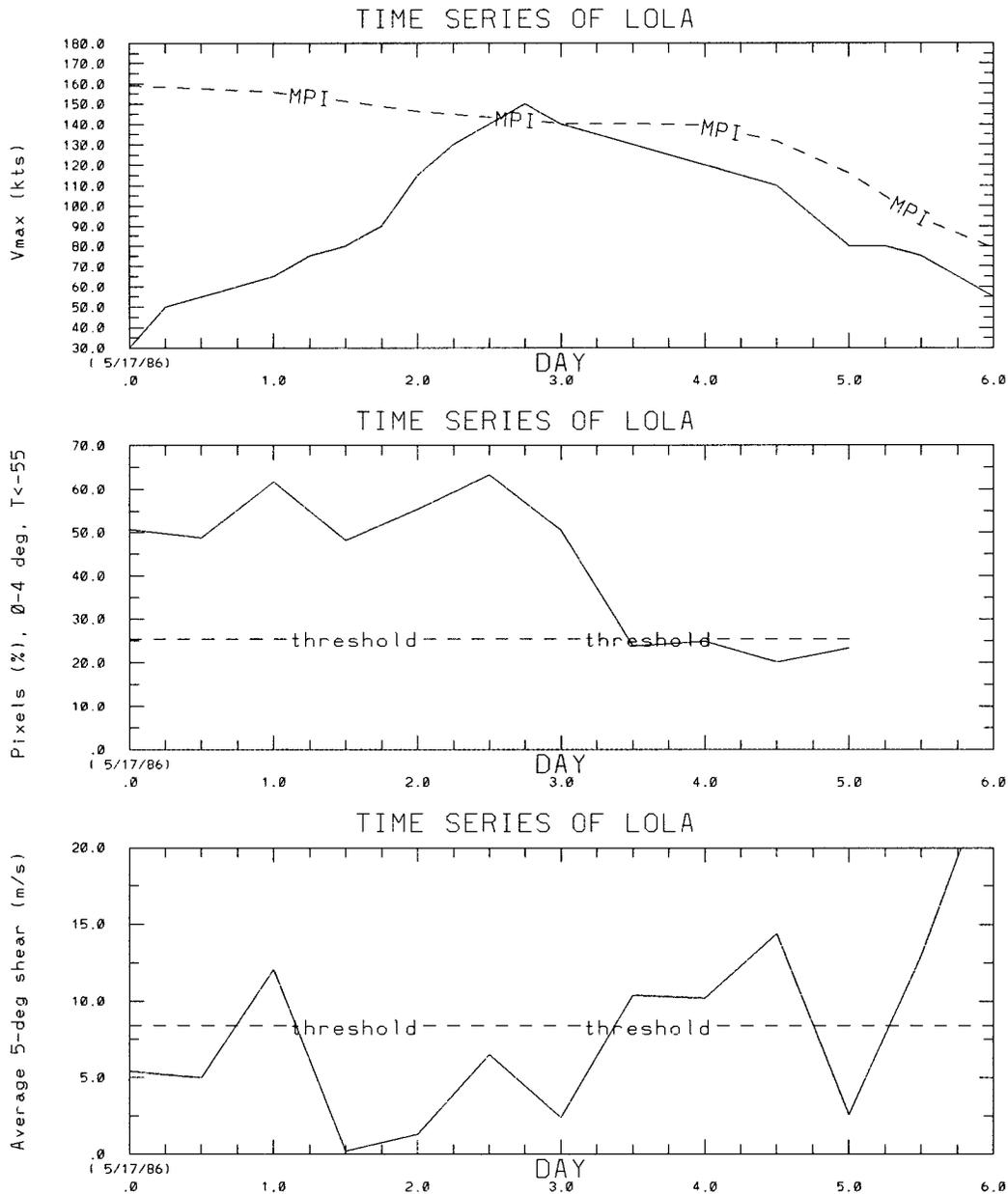| Years	$\Delta V \geq 45$	$40 \geq \Delta V \geq 20$	$15 \geq \Delta V \geq -15$	$-20 \geq \Delta V \geq -40$	$\Delta V \leq -45$	Overall
		Mean 48-h relative errors				
1984–86 TIPS	+27.0**	+7.7	−4.6***	−10.5	−10.2**	0.0**
1984–86 JTWC	+31.8	+6.0	−8.9	−9.4	−23.3	−1.7
1983 TIPS	+30.5***	+4.3***	−6.8**	−12.9	−21.2*	−1.4***
1983 JTWC	+47.1	+21.2	−1.2	−7.9	−35.8	+6.8
		Mean 48-h absolute errors				
1984–86 TIPS	27.0**	10.8***	11.4***	14.5	13.2**	13.4***
1984–86 JTWC	32.1	15.0	17.0	16.8	25.0	18.1
1983 TIPS	31.1***	10.5***	19.1	16.5	21.2*	18.4***
1983 JTWC	47.1	23.1	21.6	15.4	35.8	25.0
		No. of cases				
1984–86 cases	36	97	159	71	12	375
1983 cases	21	21	32	24	6	97

FIG. 7. Time series of MPI and V_{max} (kt, top), PX0455 with its threshold value for reference (%, middle), and VWS5 with its threshold value for reference (m s^{-1}, bottom) for Typhoon Lola (1986).

VWS5 and PX0455 from Table 4 are also included in the plots for reference.

Typhoon Lola experienced fast deepening starting day 1 since all the conditions were extremely favorable: VWS5 approached zero, PX0455 remained high at 62% (2.3 NSD), warm SSTs of 29°C supported large potential for growth (POT = 44 m s^{-1}), and a history of development (persistence) with eye formation initiated when V_{max} became faster that 55 kt. In fact, Lola managed the rare feat of reaching its MPI due to the favorable environment. Lola then began to weaken on day 3 as the water became cooler (note decrease in MPI in Fig. 7)

and shear increased with a marked decrease in convection.

Of course, fast intensification can be suppressed even with strong convective signals if the shear increases, as in the case of Hope (1985) in Fig. 8. Hope was primed for fast intensification on days 1–2 with all factors highly favorable. But on days 2.5–3.5, VWS5 became greater than 20 m s^{-1}, and intensification halted. Then Hope moved over colder waters with marginally unfavorable shear conditions and dissipated.

To further emphasize the importance of convection, Fig. 9 shows a case (Pat 1985) where the shear was very low

TIME SERIES OF HOPE

TIME SERIES OF HOPE

TIME SERIES OF HOPE

FIG. 8. As in Fig. 7 but for Typhoon Hope (1985).

($\approx$3 m s^{-1}) throughout the life cycle, but never developed much convection even though SSTs are 28°–28.5°C, and as a result intensified at a slow rate over a 3-day period to a maximum of 95 kt on day 3.5. Pat then weakened as it made landfall over southwestern Japan.

Finally, if a storm encounters strong shear after genesis such that no convection persists, little intensification will ever occur, as shown for Skip (1985) in Fig. 10. Skip persists due to warm SSTs of 28.25°–28.5°C, but except for day 3.5 encounters shear much greater than the threshold of 8.5 m s^{-1}. As a result, convection always remained below the intensification threshold.

6. Summary

A multiple regression scheme with intensity change ΔV_{max} as the dependent variable was developed for the western North Pacific Ocean. The new scheme is titled the Typhoon Intensity Prediction Scheme (TIPS). Out of 110 possible climatology, persistence, satellite, and synoptic predictors, stepwise regression was applied with a "filtering" procedure and a strict 99% significance level to reduce artificial skill and multicollinearity. This methodology yielded five to six final predictors for forecast periods of 12, 24, 36, and 48 h.

TIME SERIES OF PAT

TIME SERIES OF PAT

TIME SERIES OF PAT

FIG. 9. As in Fig. 7 but for Typhoon Pat (1985). Here, "L" denotes land interaction on day 4.

The significant predictors for all forecast periods are 1) an SST term based on the storm's "potential" for intensification (POT), which is averaged along the future storm track; 2) a binary 12-h persistence term with an "eye parameterization" (EYEPER); 3) pixel count terms within 4°; and 4) wind shear in a 5° circle averaged along the future storm track. In addition, the previous 12-h convective trend ($T_b < -65°C$) within 1° is significant for 12-h forecasts (DPX0165), meridional storm motion (VSPD) is significant except for 48-h forecasts, and storm longitude is important for 48-h forecasts. All significant predictors are positively correlated with ΔV_{max} except wind shear.

A normalization procedure allows one to infer the importance of each significant predictor, which shows the SST term (POT) to be two to three times as important as other terms, and the pixel count information to be second in importance followed by wind shear, persistence with an eye parameterization, pixel count trend, storm motion, and longitude. The normalization procedure also provides operational forecasters useful threshold values.

The total variance (R^2) of intensity change explained by TIPS is 46% at 12 h and increases with each forecast interval to 60% at 48 h. This multiple regression procedure appears to be a much better approach in TC

TIME SERIES OF SKIP

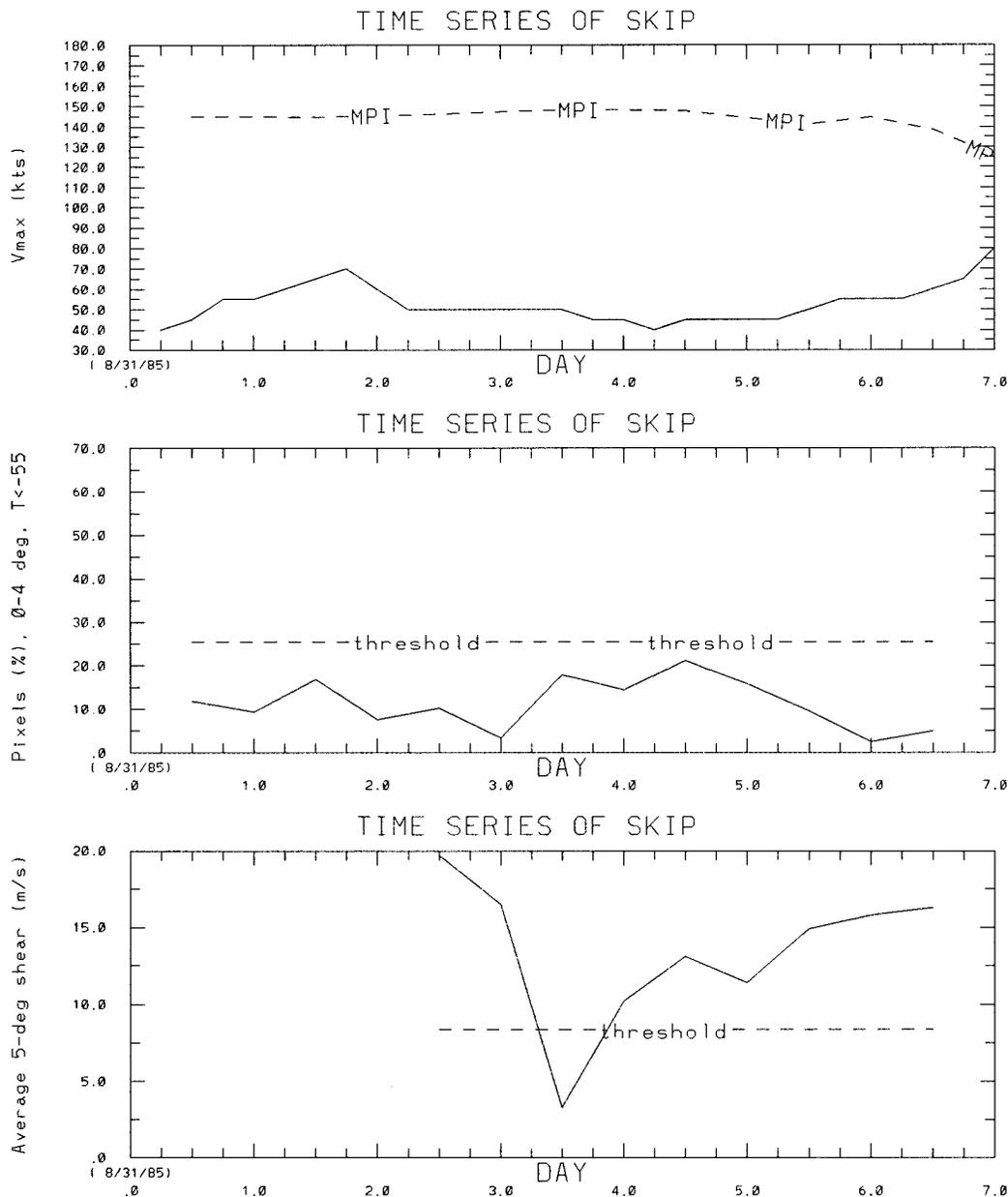## TIME SERIES OF SKIP

TIME SERIES OF SKIP

FIG. 10. As in Fig. 7 but for Typhoon Skip (1985). VWS5 was not available on days 0–2.0 and on day 7 since the TC was located east of 175°E and 5° averaged shear could not be computed in the BMRC dataset (which is restricted to 180°).

intensity change analysis than single-variable linear regression. The variance explained by any single variable alone is relatively small, indicating that TC intensity change is dependent on a combination of many factors.

Sensitivity tests showed that pixel counts in a 4° area with a brightness temperature less than −55°C (PX0455) explained 2%–3% more variance than other pixel count possibilities, possibly because it contains deep inner-core convection, is a measure of cloud symmetry, and indicates a strong secondary circulation. The 4° pixel count variable may also explain more R^2 compared to 1° and 2° pixel count variables due to positioning errors of the TC center.

Sensitivity tests also showed that averaging wind shear over a 5° area was the best shear predictor, consistent with SHIPS (DeMaria and Kaplan 1994b). Averaging shear over several data points may be more sensitive to shear impinging on the edge of the TC, and it may reduce erroneous wind observations, bogused vortexes associated with some models, and other large-scale TC circulations from contaminating the shear calculations.

While the significant predictors are of most concern in this paper, it was equally illuminating which predictors were not significant, especially since many of the unchosen potential predictors are considered to be important to TC intensity change by some researchers. The upper-level forcing terms relative eddy angular momentum flux convergence and 200-mb vorticity advection were statistically insignificant in the regression analysis. Other insignificant variables that are frequently cited in the literature, or used in some empirical schemes, are planetary eddy angular momentum flux convergence, storm speed anomaly, latitude, and the ratio of inner- to outer-core convection.

Stratifications by intensity change showed that the pixel count information provides essential information to distinguish between TCs that will intensify rapidly and those that will intensify at a slower rate, while shear and intensification potential based on SST (POT) cannot infer these differences. This implies that buoyancy is playing an important role in the intensification process and that factors that affect buoyancy require more research. On the other hand, POT and shear do provide key information between forecasting slow and fast weakening, while pixel counts do not. The contributions by other significant predictors were also discussed.

An evaluation of TIPS against the Joint Typhoon Warning Center suggests that the scheme is possibly competitive with the operational forecasts issued in 1983. However, the regression scheme still suffers large errors and underforecasts the magnitude of ΔV_{max} in fast intensification and fast weakening situations. Future possible work includes enlarging the dataset, improving the current predictors, and investigating other empirical schemes besides least squares. It is recommended that pixel counts be included in other empirical schemes that forecast TC intensification, such as SHIPS. The diabatic initialization of TC numerical models using pixel counts as done in Kasahara et al. (1996) should also be investigated. It is recommended that TIPS be tested as forecast guidance at the Joint Typhoon Warning Center. Given the scarcity of data in the Tropics, the utilization of quantitative satellite information offers some of the most hope for understanding and forecasting TC intensity change.

APPENDIX

Sensitivity Experiments of Pixel Counts and Vertical Wind Shear

During the development of TIPS, many sensitivity experiments were performed on pixel count and wind shear variables during the screening phase. These results are detailed in Fitzpatrick (1996) and summarized here. They were compared to each other in terms of mean absolute error and R^2.

The first trial replaced PX0455 with its highly correlated inner-core counterparts PX0255, PX0265, PX0155, and PX0165. Since it was possible that nonlinear satellite data will correlate better with ΔV_{max} tests were also performed on their squared counterparts. Finally, since running means are used in some operational settings, PX0455 was replaced by its 6-, 12-, and 24-h running means to assess any forecast differences.

In general, a 1%–3% reduction in R^2 occurs for all pixel count variables compared to PX0455. The absolute errors were marginally larger (0.1–1.2 kt) in most comparisons as well. PX0255, and the squared variables PX0455**2 and PX0255**2, contained the closest R^2 and absolute mean error compared to PX0455. It is interesting that in both the linear and nonlinear cases the best T_b threshold is $-55°C$, perhaps because the warmer cloud tops contain a stronger signal due to their longevity compared to higher cloud tops with a shorter, unresolved life span.

It is possible that another pixel count variable could be more statistically important than PX0455 in a different sample. It certainly is not clear that 4° storm-centered pixel counts are superior to 1° or 2° pixel count variables. The reduced R^2 may be due to errors in positioning the center of a TC to the satellite data. However, positioning errors will occur in an operational setting as well. Therefore, this analysis suggests PX0455 is the best satellite regression predictor for intensity change until proven otherwise by a better dataset or better empirical scheme.

Running means also show a degradation in R^2 of

0.5%–1.5% at 24 and 48 h compared to the observed 4° pixel counts. Mean absolute errors are essentially the same as PX0455. The least degradation occurs with the 12-h running means. This evidence suggests that temporal smoothing of the satellite data removes vital predictive signals retained at $t = 0$ and that they do not substantially improve the forecasts (with degradation more likely). It is recommended that TC intensity change schemes that use running means be reevaluated.

Sensitivity experiments were performed with point wind shear (VWSPT), averaged wind shear in a 2.5° circle (VWS2), and averaged wind shear in a 5° circle (VWS5). The variance explained by substituting VWS2 for VWS5 was 0.5% less out to 36 h, and 1% at 48 h. The variance explained by substituting VWSPT for VWS5 was 1.3% less for 12 h, increasing to 1.7% at 48 h. An interesting result is that the VWS5 threshold of 8.5 m s^{-1} increases to 9.0 m s^{-1} for VWS2 and to 9.5 m s^{-1} for VWSPT. This agrees qualitatively with Zehr's (1992) 12.5 m s^{-1} threshold for single-point shear in his tropical cyclogenesis work.

REFERENCES

Aczel, A. D., 1989: *Complete Business Statistics.* Richard D. Irwin, 1056 pp.

Chu, J., 1994: A regression model for the western North Pacific tropical cyclone intensity forecast. Tech. Rep. NRL/MR/7541-94-7215, 33 pp. [Available from Naval Research Laboratory, Monterey, CA 93943.]

Davidson, N. E., and B. J. McAvaney, 1981: The ANMRC tropical analysis scheme. *Aust. Meteor. Mag., 29,* 155–168.

DeMaria, M., and J. Kaplan, 1994a: Sea surface temperature and the maximum intensity of Atlantic tropical cyclones. *J. Climate, 7,* 1324–1334.

——, and ——, 1994b: A Statistical Hurricane Intensity Prediction Scheme (SHIPS) for the Atlantic Basin. *Wea. Forecasting, 9,* 209–220.

——, J. Baik, and J. Kaplan, 1993: Upper level eddy angular momentum flux and tropical cyclone intensity change. *J. Atmos. Sci., 50,* 1133–1147.

Dunnavan, G. M., 1981: Forecasting intense tropical cyclones using 700 mb equivalent potential temperature and central sea level pressure. NAVOCEANCOMCEN/JTWC Tech. Note 81-1, 12 pp. [Available from FPO, San Francisco, CA 96630.]

Dvorak, V. F., 1975: Tropical cyclone intensity analysis and forecasting from satellite imagery. *Mon. Wea. Rev., 103,* 420–430.

——, 1984: Tropical cyclone intensity analysis using satellite data. NESDIS 11, NOAA Tech. Memo., 47 pp. [Available from National Environmental Satellite, Data, and Information Service, Washington, DC 20233.]

Edwards, A. L., 1984: *An Introduction to Linear Regression and Correlation.* W. H. Freeman, 206 pp.

Elsberry, R. L., and R. A. Jeffries, 1996: Vertical wind shear influences on tropical cyclone formation and intensification during TCM-92 and TCM-93. *Mon. Wea. Rev., 124,* 1374–1387.

——, G. G. Coltrane, and P. L. Krueger, 1975: Statistical forecasts of 24, 48, and 72 h typhoon and tropical storm intensity changes. *J. Appl. Meteor., 14,* 445–451.

——, E. L. Weniger, and D. H. Meanor, 1988: A statistical tropical cyclone intensity forecast technique incorporating environmental wind and vertical shear information. *Mon. Wea. Rev., 116,* 2142–2154.

——, G. Holland, H. Gerrish, M. DeMaria, and C. P. Guard, 1992: Is there any hope for tropical cyclone intensity prediction?—A panel discussion. *Bull. Amer. Meteor. Soc., 73,* 264–275.

Evans, J. L., 1993: Sensitivity of tropical cyclone intensity to sea surface temperature. *J. Climate, 6,* 1133–1140.

Fitzpatrick, P. J., 1996: Understanding and forecasting tropical cyclone intensity change. Dept. of Atmospheric Sci. Paper No. 598, Colorado State University, 346 pp. [Available from Dept. of Atmospheric Sci., Colorado State University Fort Collins, CO 80523.]

——, J. A. Knaff, C. W. Landsea, and S. V. Finley, 1995: Documentation of a systematic bias in the Aviation model's forecast of the Atlantic Tropical Upper-Tropospheric Trough: Implications for tropical cyclone forecasting. *Wea. Forecasting, 10,* 433–446.

Gentry, R. C., E. B. Rodgers, J. Steranka, and W. E. Shenk, 1980: Predicting tropical cyclone intensity change using satellite measured equivalent blackbody temperatures of cloud tops. *Mon. Wea. Rev., 108,* 445–455.

Hallin, S. C., 1991: Diurnal variations in tropical cyclones. M.S. thesis, Dept. of Atmospheric Science, Colorado State University, 99 pp. [Available from Dept. of Atmospheric Science, Colorado State University, Fort Collins, CO 80523.]

Handel, M. D., 1990: Tropical cyclone intensification from finite amplitude disturbances. Ph.D. dissertation, Center for Meteorology and Physical Oceanography, Massachusetts Institute of Technology, 261 pp. [Available from Center for Meteorology and Physical Oceanography Massachusetts Institute of Technology Cambridge, MA 02139.]

Hobgood, J. S., 1986: A possible mechanism for the diurnal oscillations of tropical cyclones. *J. Atmos. Sci., 43,* 2901–2922.

Holland, G. J., 1997: The maximum potential intensity of tropical cyclones. *J. Atmos. Sci., 54,* 2519–2541.

——, and R. T. Merrill, 1984: On the dynamics of tropical cyclone structure changes. *Quart. J. Roy. Meteor. Soc., 110,* 723–745.

Holliday, C. R., and A. H. Thompson, 1979: Climatological characteristics of rapidly intensifying storms. *Mon. Wea. Rev., 107,* 1022–1034.

Jarvinen, B. R., and C. J. Neumann, 1979: Statistical forecasts of tropical cyclone intensity. NWS NHC-10, NOAA Tech. Memo., 22 pp. [Available from National Center for Environmental Prediction, Camp Springs, MD 20746.]

Kasahara, A., J. Tsutsui, and H. Hirakuchi, 1996: Inversion methods of three cumulus parameterizations for diabatic initialization of a tropical cyclone model. *Mon. Wea. Rev., 124,* 2304–2321.

Kubat, G. B., 1995: Tropical cyclone intensity relationships. M.S. thesis, Dept. of Atmospheric Science, Colorado State University, 86 pp. [Available from Dept. of Atmospheric Science, Colorado State University, Fort Collins, CO 80523.]

Martin, J. D., and W. M. Gray, 1993: Tropical cyclone observation and forecasting with and without aircraft reconnaissance. *Wea. Forecasting, 8,* 519–532.

Mayfield, M., L. Avila, and E. N. Rappaport, 1994: Atlantic hurricane season of 1992. *Mon. Wea. Rev., 122,* 517–538.

McBride, J. L., and G. J. Holland, 1987: Tropical cyclone forecasting: A world-wide summary of techniques and verification statistics. *Bull. Amer. Meteor. Soc., 68,* 1230–1238.

Merrill, R. T., 1987: An experiment in statistical prediction of tropical cyclone intensity change. NWS NHC-34, NOAA Tech. Memo., 34 pp. [Available from National Center for Environmental Prediction, Camp Springs, MD 20746.]

——, 1988: Environmental influences on hurricane intensification. *J. Atmos. Sci., 45,* 1678–1687.

Mielke, P. W., K. J. Berry, C. W. Landsea, and W. M. Gray, 1996: Artificial skill and validation in meteorological forecasting. *Wea. Forecasting, 11,* 153–169.

Molinari, J., and D. Vollaro, 1989: External influences on hurricane intensity. Part I: Outflow layer eddy angular momentum fluxes. *J. Atmos. Sci., 46,* 1093–1105.

——, and ——, 1990: External influences on hurricane intensity. Part

II: Vertical structure and response of the hurricane vortex. *J. Atmos. Sci.,* **47,** 1902–1918.

Montgomery, M. T., and B. F. Farrell, 1993: Tropical cyclone formation. *J. Atmos. Sci.,* **50,** 285–310.

Mundell, D. B., 1990: Prediction of tropical cyclone rapid intensification events. M.S. thesis, Dept. of Atmospheric Science, Colorado State University, 186 pp. [Available from Dept. of Atmospheric Science Colorado State University, Fort Collins, CO 80523.]

National Disaster Survey Report, 1993: Hurricane Andrew: South Florida and Louisiana, August 23–26, 1992. NOAA Tech. Rep., 131 pp. [Available from National Center for Environmental Prediction, Camp Springs, MD 20746.]

Neumann, C. J., 1991: A revised National Hurricane Center NHC83 model (NHC90). NWS NHC-44, NOAA Tech. Memo., 35 pp. [Available from National Center for Environmental Prediction, Camp Springs, MD 20746.]

Palmén, E., 1948: On the formation and structure of tropical cyclones. *Geophysica,* **3,** 26–38.

Pfeffer, R. L., and M. Challa, 1980: Effects of eddy fluxes of angular momentum on model hurricane development. *J. Atmos. Sci.,* **37,** 1603–1618.

Pike, A. C., 1985: Geopotential heights and thicknesses as predictors of Atlantic tropical cyclone motion and intensity. *Mon. Wea. Rev.,* **113,** 931–939.

Reynolds, R. W., 1988: A real-time global sea surface temperature analysis. *J. Climate,* **1,** 75–86.

Riehl, H., 1954: *Tropical Meteorology.* McGraw-Hill, 392 pp.

Rodgers, E. B., and H. F. Pierce, 1995: Environmental influence on Typhoon Bobbie's precipitation distribution. *J. Appl. Meteor.,* **34,** 2513–2532.

——, S. W. Chang, J. Stout, and J. J. Shi, 1991: Satellite observations of variations in tropical cyclone convection caused by upper-tropospheric troughs. *J. Appl. Meteor.,* **30,** 1163–1184.

Sadler, J. C., 1978: Mid-season typhoon development and intensity changes and the Tropical Upper Tropospheric Trough. *Mon. Wea. Rev.,* **106,** 1137–1152.

Shapiro, L. J., and C. J. Neumann, 1984: Sampling errors in statistical models of tropical cyclone motion: A comparison of predictor screening and EOF techniques. *Mon. Wea. Rev.,* **112,** 1378–1388.

Shay, L. K., P. G. Black, A. J. Mariano, J. D. Hawkins, and R. L. Elsberry, 1992: Upper ocean response to Hurricane Gilbert. *J. Geophys. Res.,* **97,** 20 227–20 248.

Sheets, R. C., 1994: Catastrophic hurricanes may become frequent events in Caribbean and along the United States East and Gulf Coast. *Hurricanes of 1992—Lessons Learned and Implications for the Future,* R. A. Cook and M. Soltani, Eds., American Society of Civil Engineers, 37–51.

Shi, J., S. W. Chang, and S. Raman, 1990: A numerical study of the outflow layer of tropical cyclones. *Mon. Wea. Rev.,* **118,** 2042–2055.

Steranka, J., E. B. Rodgers, and R. C. Gentry, 1986: The relationship between satellite measured convective bursts and tropical cyclone intensification. *Mon. Wea. Rev.,* **114,** 1539–1546.

Weatherford, C. L., 1989: The structural evolution of typhoons. Dept. Atmospheric Sci. Paper No. 446, Colorado State University, 198 pp. [Available from Dept. of Atmospheric Sci., Colorado State University, Fort Collins, CO 80523.]

——, and W. M. Gray, 1988: Typhoon structure as revealed by aircraft reconnaissance. Part I: Data analysis and climatology. *Mon. Wea. Rev.,* **116,** 1032–1043.

Willoughby, H. E., 1990: Temporal changes of the primary circulation in tropical cyclones. *J. Atmos. Sci.,* **47,** 242–264.

Zehr, R. M., 1992: Tropical cyclogenesis in the western North Pacific. NESDIS 61, NOAA Tech. Rep., 181 pp. [Available from National Environmental Satellite, Data and Information Service, Washington, DC 20233.]